Journal of Marine Science and Application (2026) 25: 162-174
https://doi.org/10.1007/s11804-025-00701-9

RESEARCH ARTICLE

Horizontal Bearing Capacity of Monocolumn Composite Bucket Foundations for Offshore Wind Turbines

Hongyan Ding[1], Renhao Wang[1], Puyang Zhang[1] and Conghuan Le[1]

Received: 29 September 2024 / Accepted: 26 February 2025

Abstract

Monocolumn composite bucket foundation is a new type of offshore wind energy foundation. Its bearing characteristics under shallow bedrock conditions and complex geological conditions have not been extensively studied. Therefore, to analyze its bearing characteristics under complex conditions—such as silty soil, chalky soil, and shallow bedrock—this paper employs finite element software to establish various soil combination scenarios. The load–displacement curves of the foundations under these scenarios are calculated to subsequently evaluate the horizontal ultimate bearing capacity. This study investigates the effects of shallow bedrock depth, the type of soil above the bedrock, the thickness of layered soil, and the quality of layered soil on the bearing characteristics of the monocolumn composite bucket foundation. Based on the principle of single-variable control, the ultimate bearing capacity characteristics of the foundation under different conditions are compared. The distribution of soil pressure inside and outside the bucket wall on the compressed side of the foundation, along with the plastic strain of the soil at the base of the foundation, is also analyzed. In conclusion, shallow bedrock somewhat reduces foundation bearing capacity. Under shallow bedrock conditions, the degree of influence on foundation bearing capacity characteristics can considerably vary on different upper soils. The thickness of each soil layer and the depth to bedrock in stratified soils also affect the bearing capacity of the foundation. The findings of this paper provide a theoretical reference for related foundation design and construction. In practice, the bearing performance of the foundation can be enhanced by improvingthe soil quality in the bucket, adjusting the penetration depth, adjusting the percentage of different types of soil layers in the bucket, and applying other technical construction methods.

Keywords Monocolumn composite bucket foundations; Shallow bedrock; Bearing characteristics; Offshore wind power; Silty soil; Chalky soil

1 Introduction

Offshore wind power has many unique advantages as a clean energy source. Moreover, marine wind energy is rich in resources and has great potential for development (Giddings et al., 2024; Soares-Ramos et al., 2020). At present, most offshore wind turbines use pile foundations or bucket foundations. The bucket foundation is a new type of foundation widely used domestically and internationally (Zhang et al., 2024a; Zhang et al., 2023). The monocolumn composite bucket foundation combines the advantages of monopile and bucket foundations. It has strong load-bearing performance, fast sinking and placement (Jia, 2017), and better towing performance (Zhang et al., 2024b). This foundation effectively improves the efficiency of offshore construction and is more economical. Currently, multiple units have been successfully applied in the Yangjiang wind farm (Liu et al., 2023). Figure 1 shows the construction of a monocolumn composite bucket foundation. Offshore wind power foundations primarily bear horizontal loads and bending moments, and their combined effect mainly manifests in their horizontal bearing characteristics. The offshore construction environment is complex, and the actual projects of offshore wind power foundations often face a variety of layered geological conditions. Especially in the South China Sea waters, there is a large amount of shallow bedrock geology. Therefore, studying the horizontal bearing characteristics of monocolumn composite bucket founda-

Article Highlights

- The monocolumn composite bucket foundation is a new type of offshore wind energy foundation.
- This paper investigates the adverse effects of shallow bedrock conditions on the bearing characteristics of monocolumn composite bucket foundations. It also examines the impact of various overburden types on the bearing capacity of the foundation under shallow bedrock conditions.
- The foundation bearing performance can be improved by replacing the soil in the bucket, adjusting the depth of the penetrating holding layer, and changing the ratio of soil layers in the bucket.

✉ Puyang Zhang
zpy@tju.edu.cn

[1] State Key Laboratory of Hydraulic Engineering Intelligent Construction and Operation, Tianjin University, Tianjin 300350, China

tions under different soil conditions, particularly under shallow bedrock geological conditions, is necessary (NEA, 2018).

Figure 1 Construction drawing of monocolumn composite bucket foundation

Regarding the bucket foundation, scholars have conducted relevant studies on its bearing characteristics. In Iran, some scholars have studied the vertical bearing capacity of semideep bases with skirts and proposed a new solution based on the vertical bearing capacity ratio of semideep to surface foundations, which demonstrates the efficiency of utilizing skirts (Rezazadeh and Eslami, 2020). A study based on geotechnical tests finds that the use of bucket foundations significantly improves the liquefaction resistance of the surrounding soil under seismic action (Chen et al., 2023). Some scholars find that the height of the bucket skirt and the spacing of the bucket foundation are two important factors affecting its bearing characteristics (Le et al., 2021; Mahmood et al., 2020).

A number of scholars have studied the bearing characteristics of foundations under complex geology. The interaction between piles and complex subsoils has recently been discussed. Three scenarios are examined, and two case studies are presented to demonstrate the improvement of geotechnical performance (Ebrahimipour and Eslami, 2024). In China, some scholars have studied the effect of complex soils on the bearing characteristics of various bucket foundations. They find that the ultimate bearing capacity of four-cylinder foundations for offshore wind power decreases as the thickness of the soft soil layer increases when the soft soil layer is the upper layer and sandy soil is the lower layer. The magnitude of the decrease varies approximately linearly with the thickness of the soft soil layer (Ding et al., 2020).

The monocolumn composite bucket foundation, a new type of bucket foundation under composite stress conditions, is studied. Vertical load increases the torque and horizontal bearing capacity to some extent. As the vertical load increases, the range and depth of the equivalent plastic strain zone in the soil at the bottom of the foundation expand when the structure reaches its ultimate bearing capacity (Zhang and Guo, 2024). Under the same conditions, composite buckets have a stronger torsional load capacity than single buckets (Zhang et al., 2021; Cui et al., 2024). Liu et al. (2016) designed a large composite bucket foundation model. They conducted relevant tests in silty clay and obtained research results on the soil pressure distribution, displacement change mechanism, and ultimate bearing capacity of the composite bucket foundation under horizontal load. To investigate the ability of the monocolumn composite bucket to withstand extreme environments, some scholars have simulated the deformation of the foundation under seismic conditions and compared it with the measured data onsite (Zhang and Zhang, 2023). In addition, the presence of compartmentalized plates within monocolumn composite bucket foundations is an important factor in increasing their load-bearing capacity (Cai et al., 2021; Le et al., 2013).

In this paper, the monocolumn composite bucket foundation is simulated and analyzed using finite element software ABAQUS. Different soil combinations are modeled, and their bearing performance is investigated. The bearing characteristics of the monocolumn composite bucket foundation under special working conditions, such as shallow bedrock, are analyzed. This provides a reference for the future construction and design of related foundations.

2 Finite element modeling of monocolumn composite bucket foundations

2.1 Computational model

ABAQUS finite element software is used to establish a monocolumn composite bucket foundation model with shell elements. The model is mainly composed of three parts: barrel, monocolumn, and connectors. The diameter of the bucket is 40 m, and the height of the skirt is 14 m. A 10-m diameter circular cabin and six equal-sized fan-shaped compartments are distributed around the circular cabin in the bucket. The bulkheads consist of six rectangular plates of equal size. The upper monocolumn has a diameter of 14 m and a height of 50 m. The monocolumn composite bucket foundation is considered an ideal elastic–plastic model in the calculation and is entirely made of steel. The steel has a modulus of elasticity of 206 GPa, a Poisson's ratio of 0.3, a yield strength of 345 MPa, and a density of 7850 kg/m³ (6850 kg/m³ underwater).

Figure 2 shows the overall calculation model of the foundation. Solid elements are used to simulate the soil body, which has a cylindrical shape with a diameter of 150 m and a thickness of 50 m. The outer edge of the foundation is 55 m away from the outer edge of the soil body, which can eliminate the boundary effect. The contact mode between each part of the foundation is set as tie contact. The contact between the foundation bucket and the soil body is set as frictional contact with a friction coefficient of 0.3.

In the finite element computational models, the founda-

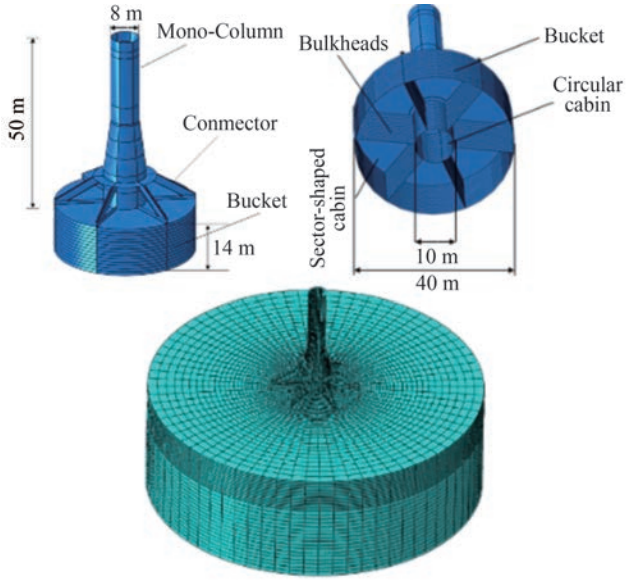

Figure 2 Finite element model

tion is simulated using S4R elements, and the soil body inside and outside the foundation is simulated using C3D8R elements. In all models, the mesh count for the monocolumn composite bucket foundation is 8 363, the mesh count for the soil body ranges from 110 956 to 114 196, and the total mesh count ranges from 119 319 to 122 559. The foundation mesh is uniformly divided, whereas the soil body mesh is divided with a dense top and sparse bottom, dense inside, and sparse outside. This improves computational efficiency.

The widely used Mohr–Coulomb model is applied to the principal model of soil. This allows for a more intuitive calculation process and requires fewer parameters, facilitating the acquisition and validation of soil parameters. The Mohr–Coulomb model accurately describes the shear failure conditions of the soil, making it particularly effective in analyzing ultimate bearing capacity. In addition, the model is applicable to offshore wind farms with a wide range of soil conditions, which are typical in such environments. This enhances the applicability of the results of this study.

2.2 Soil combinations used in the calculations

Monocolumn composite bucket foundations stabilize marine structures by pressing the bucket into the soil. Their main working environments are silty soil and chalky soil. In addition, the actual project faces a shallow bedrock geological environment. In this paper, different combinations of soil layers are established to study the horizontal bearing characteristics of the monocolumn composite bucket foundation under shallow bedrock and layered soil conditions. In the calculation, only the depth of the soil layer and soil conditions are varied. The soil parameters used are provided in Table 1, with floating weights considered for the submerged portion.

2.2.1 Shallow bedrock soil combinations in soil combinations

Submarine bedrock is characterized by high elasticity modulus and shear strength. In this study, siltstone is used as submarine bedrock. To investigate the effect of shallow bedrock depth on the horizontal ultimate bearing capacity of the foundation, two geological environments with different shallow bedrock depths are established: one with an upper layer of silty soil and the other with chalky soil. These environments are called the JN and JS series models, respectively. In addition, pure silty soil (SS) and pure chalky soil (CS) conditions are added as controls. In the JN and JS series, each 2-m change in soil layer depth represents a new condition. The JN0-JN14 and JS0-JS14 series include 18 conditions in total (including controls SS and CS). The numerical portion of the name of each condition represents the distance from the bedrock surface to the bottom of the bucket skirt, and the letter portion indicates soil type. JN refers to silty upper soil above siltstone, whereas JS refers to CS above siltstone. For example, JN4 indicates silty soil as the upper layer and a bedrock surface located 4 m below the bottom of the bucket skirt. With a bucket skirt depth of 14 m, and the bedrock is located 18 m below the mud surface. Figure 3 is a schematic of this condition.

2.2.2 Layered soil–soil combinations in soil combinations

To investigate the influence of soil quality on the horizontal bearing characteristics of the foundation within the deep soil section of the bucket, this paper establishes layered soil conditions with varying soil depths. In these conditions, the sandy soil layer is set as the lowest layer, the chalky layer as the middle layer, and another silty layer as the uppermost layer. The combined thickness of the silty and chalky layers is consistently 28 m, with only the thicknesses of these individual layers varying. A change in soil layer depth of 2 m is used to define each working condi-

Table 1 Soil parameters

Name of soil layer	Elasticity model (MPa)	Floating density (kg/m^3)	Friction angle (°)	Shear strength (kPa)
Silty soil	20	960	0	20
Chalky soil	50	1000	33	6
Sandy soil	25	1050	10	45
Siltstone	12200	1510	29	3160000

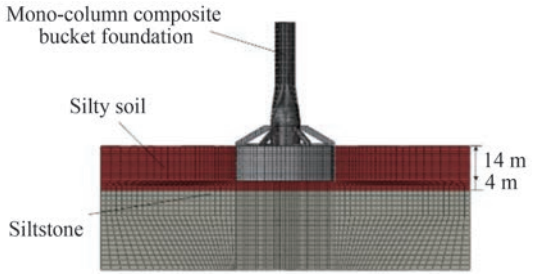

Figure 3 Schematic of JN4 working condition

tion, resulting in 15 conditions, labeled D14-0-U14. In this labeling, numbers represent the distance from the soil layer boundary to the bottom of the bucket skirt, whereas letters indicate the relative position of the boundary and the skirt bottom: "U" indicates the dividing line is above the skirt, and "D" indicates it is below. For example, U6 means that the soil layer boundary is located 6 m above the bottom of the bucket skirt, which places it 8 m below the mud surface. Under this condition, the soil layers consist of 8 m of silty soil, 20 m of CS, and 22 m of sandy soil in sequence. Figure 4 shows schematics of several typical working conditions.

2.3 Loading method

In order to investigate the ultimate bearing capacity of the model under different soil conditions, a displacement control method is used for loading. A reference point is set at the top center flange of the single column of the foundation, which is coupled with the model. A horizontal displacement of 3 m along the *x*-axis is applied at this reference point, directing the load in a single direction. The displacement–load curve of the foundation is then calculated to analyze its ultimate bearing capacity. The loading method is shown in Figure 5.

2.4 Model verification

To verify the convergence and accuracy of the finite element model, grid sensitivity analysis is conducted, focusing on critical regions such as the bucket–soil interface. The analysis aimed to ensure that the results are independent of mesh size and that the model behaves consistently under varying mesh densities.

The finite element model used to calculate the 0-condition is selected and analyzed with three different mesh densities: coarse mesh, medium mesh, and fine mesh. The total number of elements in these cases is 82 867 (5 538 for the foundation), 122 559 (7 020 for the foundation), and 180 817 (10 296 for the foundation), respectively. The corresponding calculated bearing capacities are 34.33 MN, 34.23 MN, and 34.30 MN. The negligible variation between medium and fine meshes confirmed convergence. Similar trends were observed across other conditions.

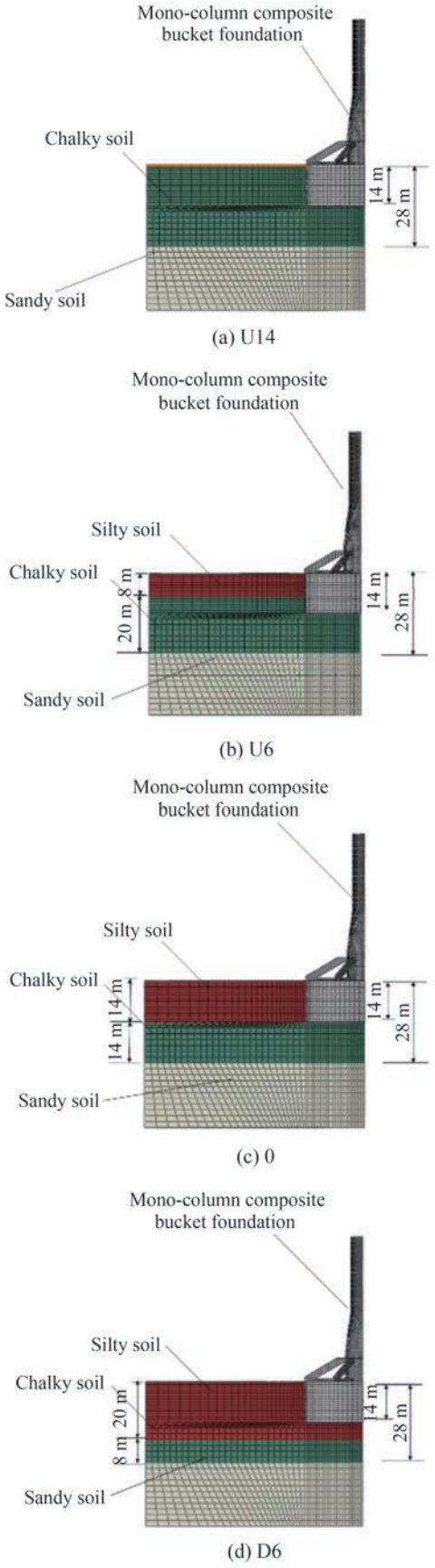

Figure 4 Schematic of some working conditions

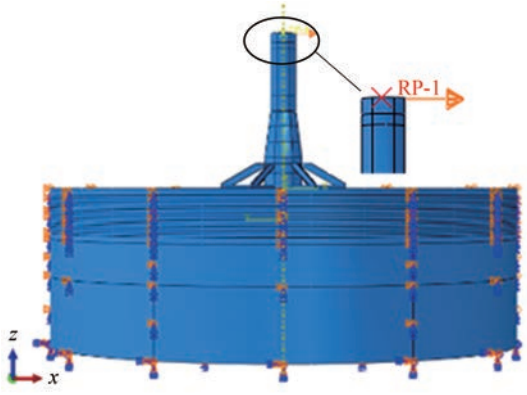

Figure 5 Schematic of loading method

3 Calculation results and analysis

3.1 Method of determining the horizontal ultimate bearing capacity

The horizontal ultimate bearing capacity of the foundation can be determined from the load–displacement curve. If there are extreme points on this curve, the load at the first extreme point represents the ultimate bearing capacity of the foundation. As shown in Figure 6, if the curve lacks a distinct inflection or an extreme point, the tangent intersection method can be used. In this method, a tangent is drawn at the beginning and at the end of the load–displacement curve, and the load at the intersection of these two tangents is taken as the ultimate bearing capacity of the foundation (Mosallanezhad et al., 2008).

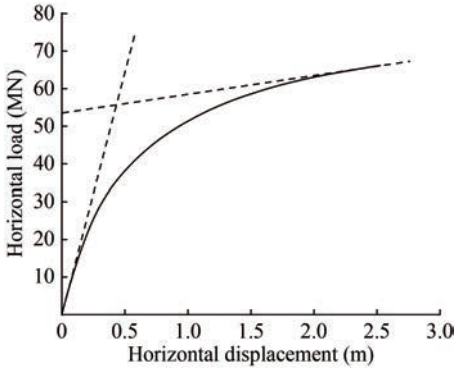

Figure 6 Determination of ultimate bearing capacity by the tangent intersection method

3.2 Analysis of calculation results

In determining the ultimate bearing capacity, only the displacement–load curves for the D14-D6 conditions show distinct extreme values. Therefore, the maximum values in these conditions are used as the calculated ultimate load capacities. For the remaining conditions, the tangent intersection method is used to determine their ultimate bearing capacity values. Table 2 presents the calculated values of the horizontal ultimate bearing capacity for all working conditions.

Table 2 Calculated value of ultimate bearing capacity

Calculation of working conditions	Relative height (m)	Bearing capacity (MN)
U	14	57.11
	12	54.25
	10	50.24
	8	45.45
	6	41.00
	4	38.30
	2	37.53
0	0	34.23
D	−2	30.40
	−4	27.62
	−6	26.84
	−8	24.74
	−10	23.09
	−12	21.73
	−14	20.78
SS	–	18.53
JN	0	34.33
	−2	30.31
	−4	27.39
	−6	25.02
	−8	23.03
	−10	21.77
	−12	20.67
	−14	19.76
JS	0	62.24
	−2	60.84
	−4	59.99
	−6	58.94
	−8	58.41
	−10	58.05
	−12	58.03
	−14	57.86
CS	–	56.92

3.2.1 Analysis of ultimate bearing capacity of working conditions of silty soil overlying shallow bedrock

As shown in Figure 7, the horizontal ultimate bearing capacity for the JN soil condition is obtained using the tangent intersection method. The load−displacement curve is

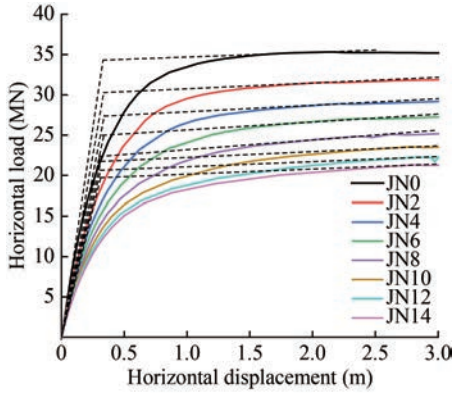

Figure 7 Displacement–load diagram of JN series

nonlinearly fitted with the Asymptotic1 model, yielding the following fit function:

$$y = 16.87 + 17.44 \times 0.88^{x} \quad (1)$$

The fitting function R^2 is 0.999 4, indicating a good fit, and the fitting curve is shown in Figure 8.

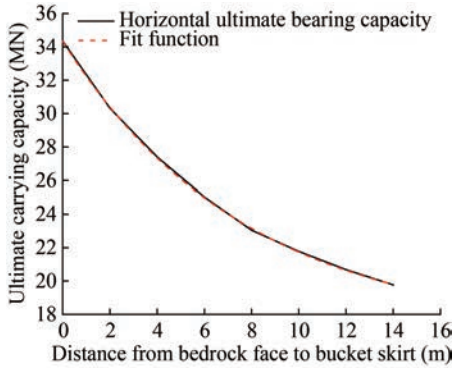

Figure 8 Ultimate bearing capacity–bucket depth curve and fitting function diagram

Part ($b \times c^x$) of Eq. (1) ($b \times c^x$ represents the part 17.44 × 0.88^x mentioned in the equation above) can be considered as the increase in the ultimate bearing capacity of the foundation as the depth to bedrock changes. In conclusion, under shallow bedrock conditions with a silty upper soil layer, the horizontal ultimate bearing capacity of the foundation increases approximately exponentially as the distance from the bedrock surface to the bottom of the bucket skirt decreases. When the bottom of the bucket skirt aligns with the bedrock surface, the foundation reaches its maximum bearing capacity. Under pure silty soil conditions, the ultimate bearing capacity is 18.53 MN. In the range of 0.5 times the bucket skirt depth from the bedrock surface to the bottom of the bucket skirt, the horizontal bearing capacity, calculated using the fitting function, exceeds 23.03 MN, which is more than 24% higher than the value under pure silty soil conditions. In the range of 1 times the bucket skirt depth, the horizontal ultimate bearing capacity exceeds 19.76 MN. The bedrock increased its horizontal bearing capacity by more than 7%. Notably, the distance from the bedrock surface to the bottom of the bucket skirt considerably affects the overburden when silty soils are used as the overburden.

3.2.2 Analysis of ultimate bearing capacity of working conditions of chalky soil over shallow bedrock

As shown in Figure 9, the horizontal ultimate bearing capacity under the JS soil condition is obtained using the tangent intersection method. A plot of the distance from the bedrock surface to the bottom of the bucket skirt versus the horizontal ultimate bearing capacity of the foundation is then obtained, with the upper soil being CS. The Asymptotic1 model is used to fit the curve nonlinearly, and the resulting fitting function is as follows.

$$y = 57.37 + 4.91 \times 0.83^{x} \quad (2)$$

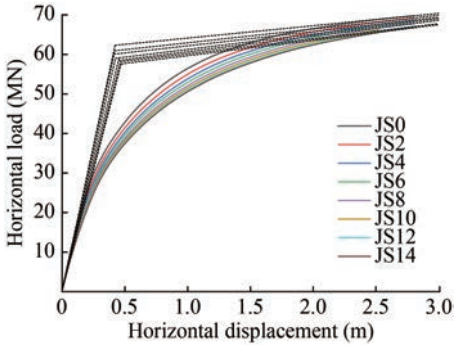

Figure 9 Displacement–load diagram of JS series

The fitting function R^2 is 0.994 5, indicating a good fit, and the fitting curve is shown in Figure 10.

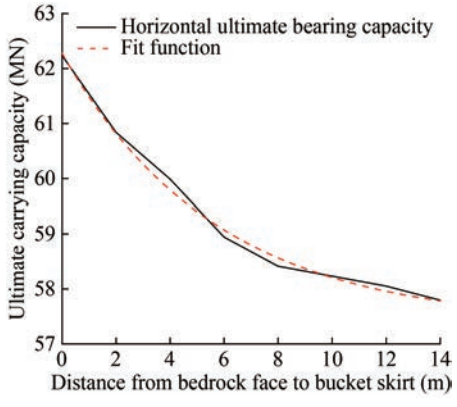

Figure 10 Ultimate bearing capacity–bucket depth curve and fitting function diagram

When the upper soil layer over shallow bedrock is CS, the horizontal ultimate bearing capacity of the foundation increases approximately exponentially as the distance

from the bedrock surface to the bottom of the bucket skirt decreases. However, the overall increment is relatively small. Under pure CS conditions, the ultimate load-bearing capacity is 56.92 MN, and when the bottom of the bucket skirt is exactly at the bedrock surface, the maximum load-bearing capacity reaches 62.24 MN, an increase of about 9.3%. In the range of 0.5 times the bucket skirt depth from the bedrock surface to the bottom of the bucket skirt, the horizontal bearing capacity is 58.41 MN, which is about 2.6% higher than the pure CS condition. Notably, the distance from the bedrock surface to the bottom of the bucket skirt has little effect on the overburdened soil in the CS condition.

For the JN (-14-0) condition and the JS (-14-0) condition, the lower soil layer consists of hard soil, whereas the upper soil layer consists of soft soil. When the soft soil layer overlying the hard soil layer is compressed, the bearing capacity formula is provided in ISO 19905-1-2023 (ISO, 2023):

$$Q_V = \left(a_s + \frac{b_s B}{T} + \frac{1.2D}{B}\right) s_u A + p_0 A \tag{3}$$

where a and b are constants. A and B are the relevant dimensions of the foundation, which are fixed values. s_u is the shear strength of the soft soil layer, which is also a fixed value. D and p_0 are the depth of the foundation and the effective soil pressure. In this study, the depth of the monocolumn composite bucket foundation remains constant at 14 m. Therefore, in the comparative analysis, p_0 also remains unchanged. T is the distance from the bottom of the bucket skirt to the soil layer demarcation line, and this value gradually decreases in the JS (-14-0) and JN (-14-0) conditions. Therefore, in conclusion, as the distance from the bottom of the bucket skirt to the soil layer demarcation line decreases, the bearing performance of the foundation will gradually improve. This is consistent with the pattern observed in the numerical simulation results of this paper.

3.2.3 Analysis of ultimate bearing capacity of working conditions of chalky soil over shallow bedrock

The displacement–load diagrams for conditions D and U are shown in Figure 11. The dotted line represents the D condition, and the solid line represents the U condition, according to the calculated data. An extreme point is observed in the load–displacement curve for the D14-D6 condition, and the load corresponding to this extreme point represents the ultimate bearing capacity of the foundation. The curve for the D4-U14 condition does not have an extreme point, and the horizontal ultimate bearing capacity is determined using the tangent line intersection method for the corresponding conditions. The relative position of the bottom of the bucket skirt, determined by the soil layer demarcation line, is taken as the horizontal coordinate, and the horizontal ultimate bearing capacity of the foundation is taken as the vertical coordinate to plot the curve shown in Figure 12.

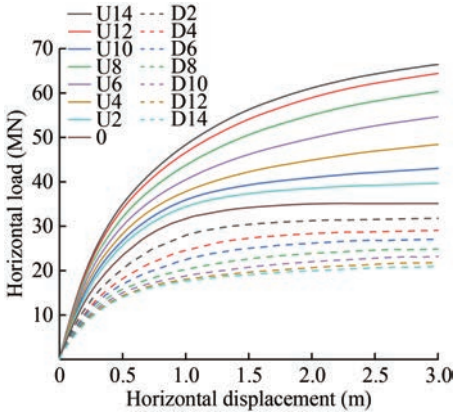

Figure 11 D–U working condition displacement–load diagram

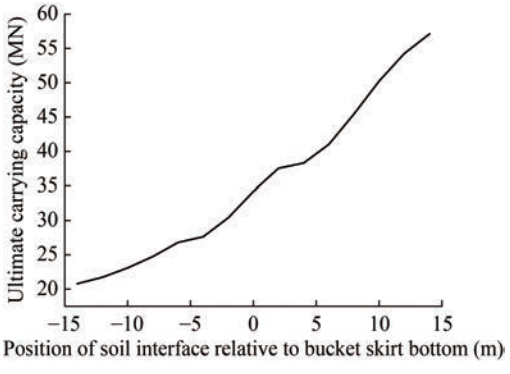

Figure 12 Ultimate bearing capacity–bucket depth relationship diagram

Notably, the load–displacement curves obtained when the composite bucket is entirely made of silty soil (D14-0) are flatter than those obtained when the bucket is mixed with CS (U2-U14). The bearing capacity of CS is clearly stronger than that of silty soil, and the ultimate bearing capacity in the (0-U14) conditions is greater than that in the (D14-D2) conditions when the bearing layer is CS.

The growth rate of bearing capacity in both cases is calculated, as shown in Figure 13. When CS is used as the lower layer, the smaller the distance from the bottom of the bucket skirt, the greater the bearing capacity of the foundation and its growth rate. When the CS layer is used as the holding layer, the more it occupies the composite bucket, the greater the bearing capacity of the foundation. The bearing capacity of the monocolumn composite bucket foundation grows the fastest when the insertion depth into the CS is within 0.5 times the height of the bucket skirt. When the insertion depth exceeds 0.7 times the height of the bucket skirt, the growth rate of the bearing capacity decreases substantially. Therefore, in construction, the height of CS in the bucket skirt should be controlled to be no more than half of the height of the bucket skirt to achieve

a more effective improvement in the bearing capacity of the foundation.

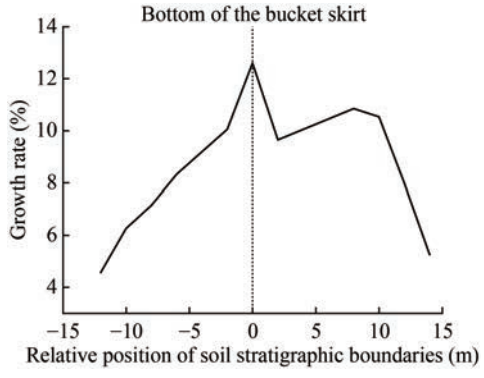

Figure 13 Growth rate–bucket depth relationship diagram

3.3 Comparative analysis of calculation results

3.3.1 Comparative analysis of calculation results for shallow bedrock conditions and layered soil conditions

The load–displacement curves and the curves of horizontal ultimate bearing capacity versus the relative position for the D-series and JN conditions are selected for comparative analysis. In both conditions, the upper soil layer is silty soil, whereas the lower soil layer consists of CS and shallow rocky foundation, respectively. As shown in Figure 14, the overall trend for both conditions is that the bearing capacity gradually increases as the distance from the soil layer demarcation line to the bottom of the bucket skirt decreases. However, the ultimate bearing capacity of the former is higher than that of the latter. In other words, under the same thickness of the holding layer and the same soil parameters, the bearing capacity in the condition with the subsoil as CS is stronger than that in the condition with the subsoil as shallow bedrock.

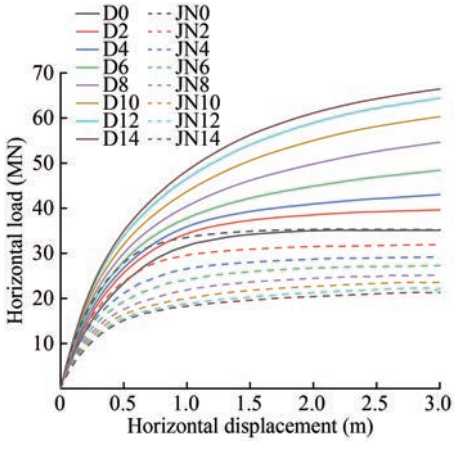

Figure 14 D–JN working condition displacement–load diagram

As shown in Figure 15, when the soil layer demarcation line is more than 0.5 times the height of the bucket skirt from the bottom of the foundation, the bearing capacity of the lower soil is significantly higher than that of the shallow rock foundation condition. If the distance is less than this range, the gap between the two conditions will rapidly decrease. When the bottom of the bucket skirt is exactly at the soil quality demarcation line, the bearing capacity reaches its maximum and nearly becomes equal for both conditions. Therefore, in the case of CS, the bottom of the bucket skirt should be kept away from the soil layer demarcation line during the foundation penetration construction. Ensuring that the bottom of the bucket skirt is at least 0.5 times the depth of the bucket skirt away from the soil layer demarcation line will fully utilize the advantages of the CS.

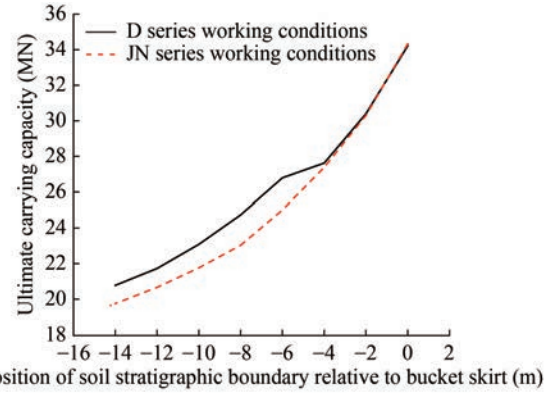

Figure 15 D–JN ultimate bearing capacity comparison chart

The damage to the soil body is analyzed when the foundation reaches its horizontal ultimate bearing capacity under the above conditions. Figure 16 shows the equivalent plastic strain diagrams of the foundation under representative ultimate moment loads for the two working conditions. These are the profiles of the planes where the forces are applied. As shown in the figure, as the relative distance of the soil layer demarcation line increases, the plastic deformation zone inside the bucket decreases, whereas the plastic deformation zone outside the bucket gradually increases. When the relative distance reaches one times the height of the bucket skirt, the thickness of the silty clay in the holding layer becomes large enough. Eventually, both zones form a coherent "V"-shaped failure surface under the bucket.

At the point where the failure surface of the clay soil reaches the soil layer demarcation line, the bedrock does not experience any plastic strain under shallow bedrock conditions. The failure surface cannot extend into deeper soil layers, and the load cannot be transferred further downward. However, in the condition where the subsoil is CS, some plastic deformation zones also appear in the subsoil, indicating that the load can be transferred further downward. In this case, more soil is mobilized and involved in bearing the load. In extreme conditions such as JN0 and D0, the failure surface appears in the CS layer in the D0 condition, but only the holding layer bears the load in the JN0 condition. This results in a situation where the shal-

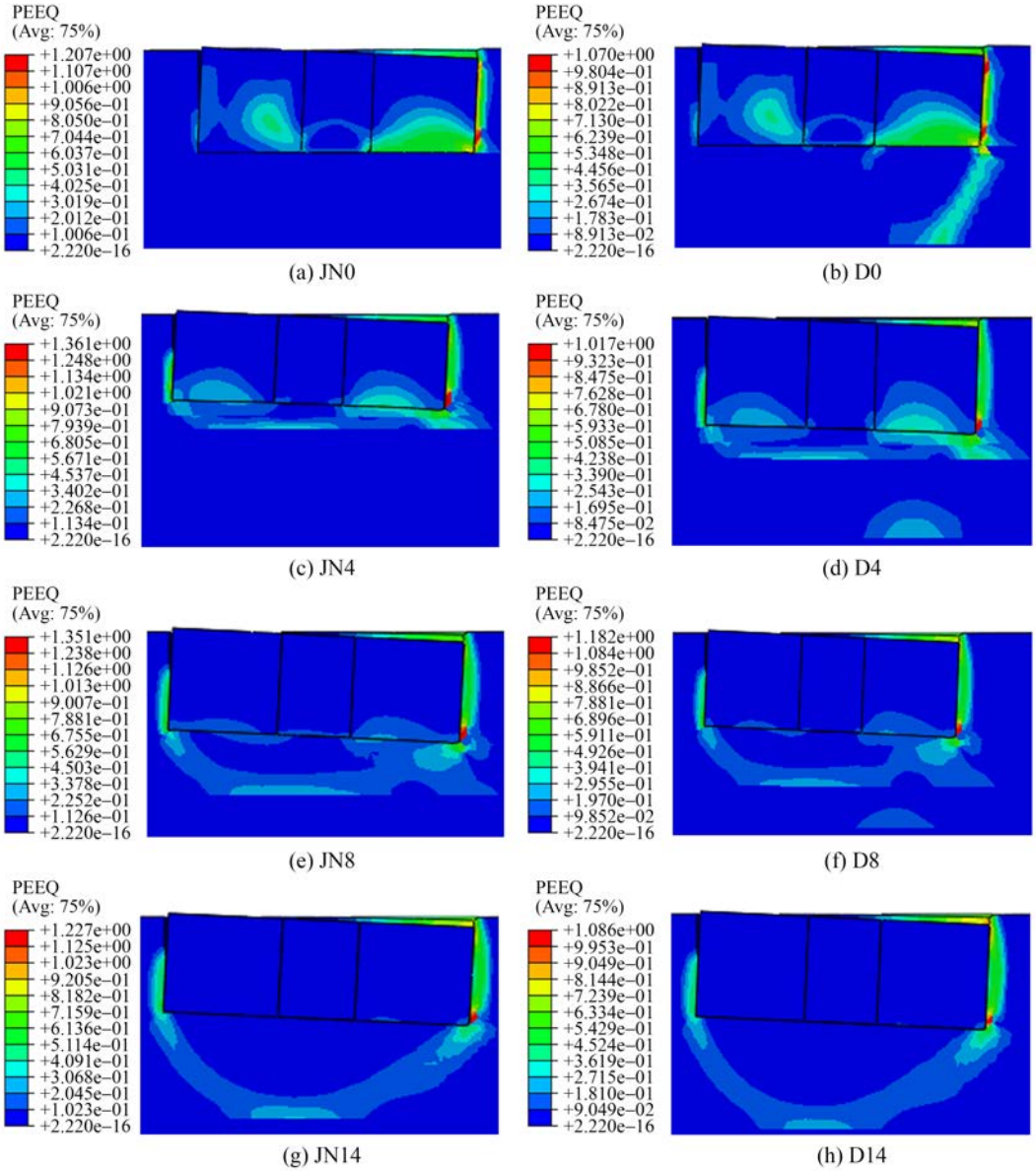

Figure 16 Equivalent plastic strain diagram of representative foundations under JN and D conditions

low bedrock soil parameters are substantially stronger than those of CS, but the bearing capacity of the foundation is always lower under shallow bedrock conditions than when the underlying soil is chalky.

As the soil parting line approaches the bottom of the bucket skirt, the plastic deformation zone in the composite bucket increases, and the percentage of the load borne by the soil inside the bucket also rises. Within a certain range, even the soil layer inside the bucket shows signs of plastic deformation. Figure 17(a) shows the upper soil displacement vector map under the SS condition, and Figure 17(b) shows the upper soil displacement vector map under the JN6 condition.

When the strength of the lower soil layer is higher than that of the upper soil layer, the lower soil layer impedes the displacement of the soil body when bearing loads to some extent. This, in turn, enhances the "soil capacity" characteristics of the foundation and improves the integrity between the soil and the foundation, resulting in a gradual increase in the bearing capacity of the foundation. This effect becomes more pronounced as the relative distance between the soil strata boundary decreases.

Figure 18 shows the soil pressure inside and outside the composite bucket on the compression side when the horizontal bearing capacity of the foundation is reached for the JN and D conditions. In Figure 18, the dashed lines represent the soil pressure changes along the depth inside and outside the bucket wall for the JN condition, whereas the solid line represents the pressure changes for the D condition. The trend of soil pressure changes inside and outside the bucket is similar for both conditions. This is because the failure surface mainly occurs in the holding layer,

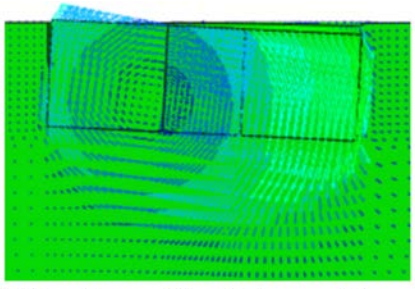

(a) SS working condition displacement diagram

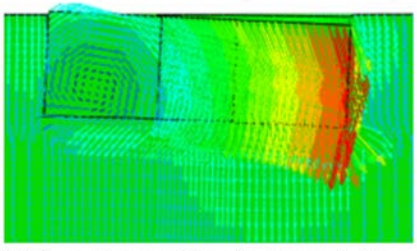

(b) JN6 working condition displacement diagram

Figure 17 Vector diagram of displacement of upper soil under SS and JN6 working conditions

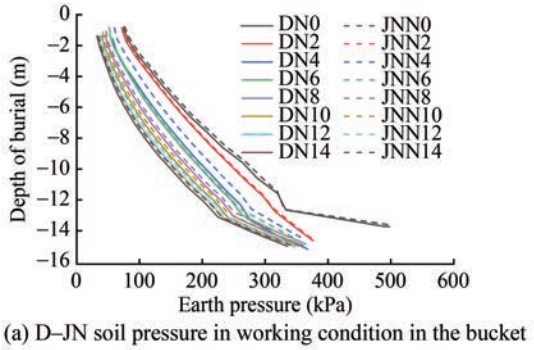

(a) D–JN soil pressure in working condition in the bucket

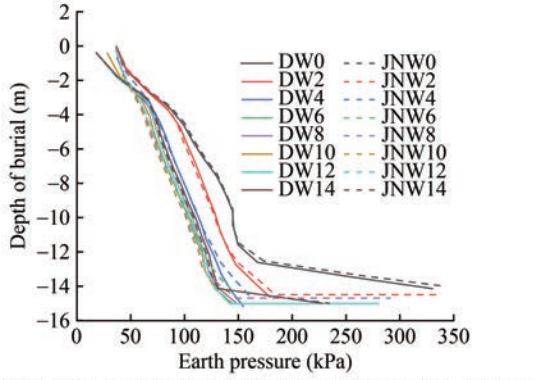

(b) D–JN soil pressure outside the working condition bucket

Figure 18 D–JN working condition soil pressure (N represents the soil pressure inside the foundation; W represents the soil pressure outside the foundation)

which is silty soil for both conditions. Therefore, when the ultimate horizontal bearing capacity is reached, the soil pressure distribution at the same depth of the soil layer demarcation line is nearly identical. As the distance between the soil layer demarcation line and the bottom of the bucket skirt decreases, the soil pressure inside and outside the bucket skirt gradually increases, indicating a corresponding improvement in load-bearing capacity.

By comparing and analyzing the two conditions, the soil pressure inside the bucket is consistently higher in the JN condition, whereas the soil pressure outside the bucket is lower overall. In the JN condition, the percentage of the load borne by the soil inside the bucket is greater than that in the D condition. The soil resistance provided by the bucket wall on the pressurized side of the foundation mainly comes from passive earth pressure, which is lower in the JN condition. As a result, the horizontal ultimate bearing capacity of the foundation is reduced in the shallow bedrock condition. The bearing capacity of the foundation relies more on the soil inside the bucket, which accounts for a larger percentage. Therefore, in the construction of shallow bedrock conditions, replacing the soil inside the bucket with better soil may be beneficial to improve the bearing capacity.

3.3.2 Comparative analysis of calculation results of different overburden conditions for shallow bedrock

The load–displacement curves for the JS and JN series working conditions, along with the horizontal ultimate bearing capacity and relative position curves, are selected for comparative analysis, as shown in Figures 19 and 20. Both conditions involve shallow bedrock, with the upper soil layers being CS and silty soil, respectively.

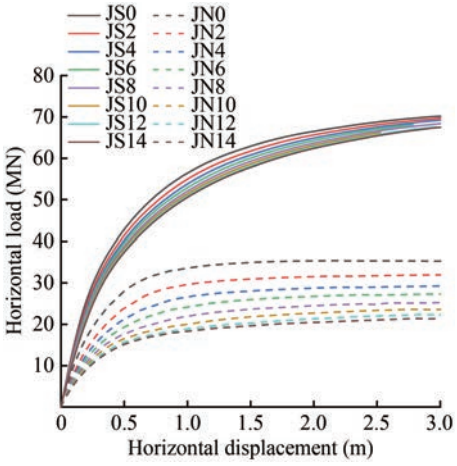

Figure 19 JS–JN working condition displacement–load diagram

The overall trend for both conditions shows a gradual increase in bearing capacity as the distance from the soil layer demarcation line to the bottom of the bucket skirt decreases. The bearing capacity of the foundation is considerably higher when the upper layer is CS than when it is silty soil. However, in silty soil conditions, the bearing capacity is more affected by the distance between the bedrock surface and the foundation, whereas in CS conditions, the bearing capacity is almost unaffected. Therefore, in conclusion, the depth of shallow bedrock affects the bearing

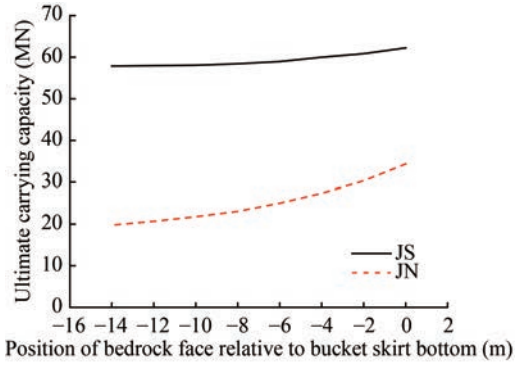

Figure 20 Comparison diagram of the JS−JN ultimate bearing capacity

characteristics of the foundation differently depending on the soil quality of the holding layer.

The damage behavior of the foundation is analyzed when it reaches the horizontal ultimate bearing capacity under the JS condition. Figure 21 shows the equivalent plastic strain diagram of the foundation under representative ultimate moment loads in the JS condition. These diagrams represent the profiles of the planes where the forces are applied. As bedrock depth increases, the plastic deformation zone within the bucket decreases, whereas the plastic deformation zone outside the bucket gradually expands. In the JS condition, the plastic zone inside the bucket essentially disappears, yet plastic deformation zones inside and outside the bucket persist. The soil inside the bucket continues to bear a remarkable portion of the load, and the plastic deformation area in the compression zone is noticeably larger than on the opposite side.

As shown in Figure 22, observing the upper soil displacement vector map, the CS condition does not create a coherent soil movement path. In the outer compression zone of the bucket, the upper part of the soil body is uplifted by compression, whereas the lower part and deeper layers of the soil body move downward. As the bedrock depth increases, the width of the upper uplifted soil region decreases, and the depth of the downward-moving soil in the lower part increases.

Figure 23 shows the soil pressure inside and outside the bucket on the compression side of the composite bucket when the foundation reaches the ultimate bearing capacity under the JN and JS conditions. The dashed line indicates the variation of soil pressure with depth inside and outside the bucket wall for the JN condition, whereas the solid line shows the soil pressure variation for the JS condition.

The changing trends of earth pressure inside the bucket are similar for both conditions. The soil pressure increases as the bucket depth increases, i.e., as the distance from the bedrock surface to the bottom of the bucket skirt decreases. However, owing to differences in soil quality, the soil pressure inside the bucket for the JN condition is much lower than that for the JS condition when the bedrock depth is the same. The earth pressure outside the bucket varies between the two conditions: under the JN condition, the earth pressure outside the bucket continuously increases with the bucket depth, with a sharp rise as the bottom of the bucket is approached. Under the JS condition, the earth pressure outside the bucket initially increases with bucket depth, then decreases, reaching its maximum when the depth is half of the bucket skirt height. The soil pressure outside the bucket is nearly symmetrically distributed around half of the bucket skirt height in the vertical direction. In the calculation range, the maximum value of soil pressure outside the bucket does not differ remarkably between the two conditions, but the difference in soil pres-

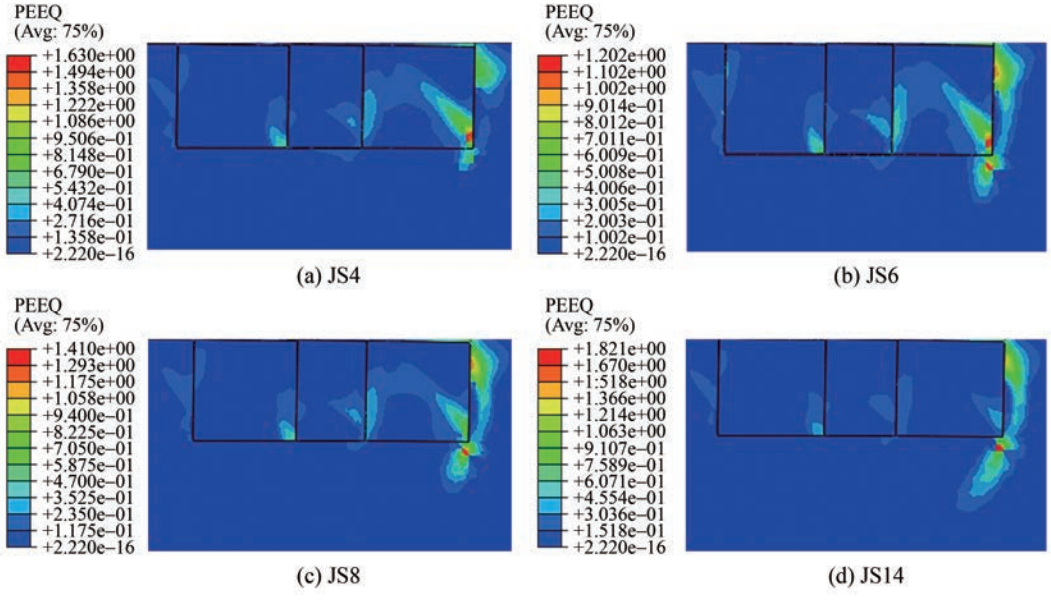

Figure 21 Equivalent plastic strain diagram of representative foundations under JS conditions

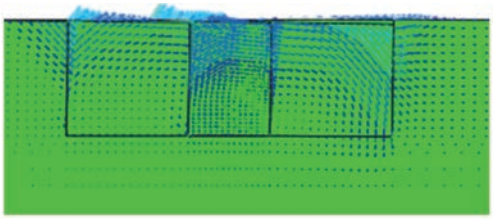

Figure 22 Vector diagram of displacement of upper soil under JS working conditions

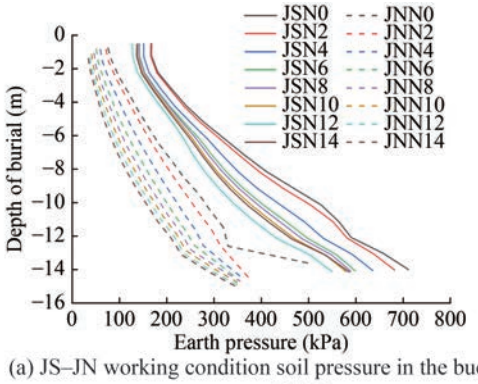

(a) JS–JN working condition soil pressure in the bucket

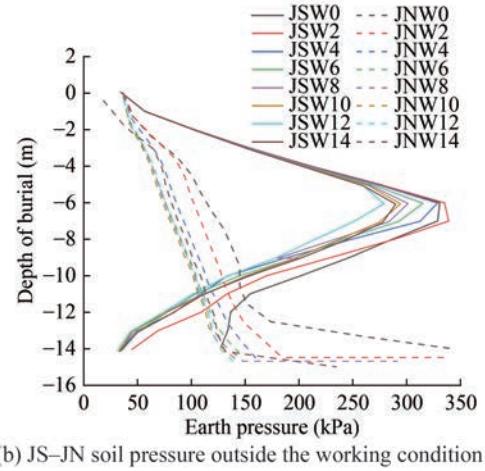

(b) JS–JN soil pressure outside the working condition bucket

Figure 23 JS–JN working earth pressure (N represents the soil pressure inside the foundation; W represents the soil pressure outside the foundation)

sure inside the bucket is more pronounced. This is attributed to the different soil qualities.

4 Conclusions

In this paper, four different series of working conditions with 33 distinct soil combinations are established using finite element analysis. This study investigates the effects of shallow bedrock depth, varying types of upper soils, and different soil qualities on the horizontal bearing characteristics of a monocolumn composite bucket foundation. The following conclusions are drawn:

1) When shallow bedrock is present below the foundation, it creates an unfavorable condition, reducing the horizontal ultimate bearing capacity of the foundation to some extent. Among all calculation conditions, the overall bearing capacity follows the order of JS > U > D > JN. The bearing capacity of the foundation is remarkably stronger when CS serves as the bearing layer compared with silty soil. The bearing performance of the foundation improves when the upper layer above the shallow bedrock is CS.

2) In shallow bedrock conditions, the relative distance between the bedrock surface and the bottom of the bucket skirt has a certain effect on the bearing capacity of the foundation. Overall, as this relative distance decreases, the bearing performance of the foundation improves to some extent. However, the degree of improvement is highly influenced by the soil quality of the upper layer, with silty soil showing a much greater enhancement effect than CS. Under shallow bedrock conditions, the bearing capacity of the foundation depends more on the proportion of soil within the bucket. Therefore, in shallow bedrock construction, replacing the bucket soil with higher-quality soil could be considered to enhance the bearing capacity of the foundation.

3) In nonshallow bedrock geological conditions, the thickness of silty soil and CS substantially impacts the bearing performance of the foundation. When the CS within the foundation bucket occupies a range of 0.5 times the depth of the bucket skirt, the foundation bearing capacity is notably enhanced. In foundation penetration construction, positioning the bottom of the bucket skirt 0.5 times the depth of the bucket skirt away from the soil layer demarcation line allows for the advantages of silty soil over shallow bedrock to be fully utilized.

4) Under the same series of working conditions, as the relative position of the soil layer demarcation line and the bottom of the bucket skirt changes, the soil pressure inside and outside the bucket wall on the pressurized side of the foundation, as well as the surrounding soil layer, exhibit consistent patterns of change. For different soil types, whether in shallow bedrock conditions, the earth pressure on the pressurized side of the bucket wall (inside and outside) and the plastic deformation zone of the surrounding soil considerably vary.

Competing interest The authors have no competing interests to declare that are relevant to the content of this article.

References

Cai Z, Wang Q, Guan Y, Han X, Li W (2021) Influences of bulkheads on bearing characteristics of composite bucket foundation of offshore wind turbines. Chinese Journal of Geotechnical Engineering 43(4): 751-759. (in Chinese) DOI: 10.11779/CJGE202104018

Chen L, Tian H, Xu M (2023) Seismic response analysis of offshore

wind power composite bucket foundation based on geotechnical test. Structural Engineers 39(6): 171-178. (in Chinese) DOI: 10.15935/j.cnki.jggcs.2023.06.019

Cui X, Shi Y, Wei X, Le C, Jiang M, Zhang P (2024) Analysis of bearing characteristics of four-bucket jacket foundation in combined loading mode. Acta Energiae Solaris Sinica 45(6): 581-588. (in Chinese) DOI:10.19912/j.0254-0096.tynxb.2023-0248

Ding H, Zhang C, Zhang P, Zhai H (2020) Effect of overlying soft soil layer on bearing capacity of four bucket foundation for offshore wind turbines. Journal of Harbin Engineering University 41(1): 67-75. (in Chinese) DOI:10.11990/jheu.201808055

Ebrahimipour A, Eslami A (2024) Analytical study of piles behavior for marine challenging substructures. Ocean Engineering 292: 116514. https://doi.org/10.1016/j.oceaneng.2023.116514

Giddings J, Bloomfield H, James R, Blair M (2024) The impact of future UK offshore wind farm distribution and climate change on generation performance and variability. Environmental Research Letters 19(6): 064022. DOI 10.1088/1748-9326/ad489b

ISO (2023) ISO 19905-1-2023. Petroleum and natural gas industries-Site-specific assessment of mobile offshore units-Part 9: Foundations. International Organization for Standardization, Geneva

Jia N (2017) Analysis on penetrating-levelling mechanism and penetration resistance of bucket foundation with inner compartments for offshore wind turbines. PhD thesis, Tianjin University, Tianjin, 4-8. (in Chinese)

Le C, Ding H, Zhang P (2013) Influences of bulkheads on the bearing mode of concrete bucket foundation for offshore wind turbine. Engineering Mechanics 39(2): 12-19. (in Chinese) DOI: 10.6052/j.issn.1000-4750.2011.05.0331

Le C, Ren J, Jiang M, Zhang P, Ding H (2021) Analysis of the moment bearing capacity of four-bucket jacket foundation in sandy soil. Ocean Engineering 39(2): 12-19. (in Chinese) https://doi.org/10.16483/j.issn.1005-9865.2021.02.002

Liu J, Ni D, Xiao J, Zhang P (2023) Analysis of penetrating process of single-column composite bucket foundation for offshore wind turbine. Acta Energiae Solaris Sinica 44(3): 239-243. (in Chinese) DOI:10.19912/j.0254-0096.tynxb.2022-0305

Liu Y, Ding H, Zhang P (2016) Model tests on bearing capacity of composite bucket foundation in clay. Chinese Journal of Geotechnical Engineering 38(12): 2315-2321. (in Chinese) DOI: 10.11779/CJGE201612022

Mahmood MR, Fattah MY, Khalaf A (2020) Experimental investigation on the bearing capacity of skirted foundations on submerged gypseous soil. Marine Georesources & Geotechnology 38(10): 1151-1162. https://doi.org/10.1080/1064119X.2019.1656311

Mosallanezhad M, Hataf N, Ghahramani A (2008) Experimental study of bearing capacity of granular soils, reinforced with innovative Grid-Anchor system. Geotechnical and Geological Engineering 26(3): 299-312. DOI: 10.1007/s10706-007-9166-z

NEA (2018) Design code for offshore wind farm turbine foundations. China Water & Power Press, Beijing, NB/T 10105-2018. (in Chinese)

Rezazadeh S, Eslami A (2020) Skirted semi-deep foundations behavior on deposits with variable undrained shear strength. Ships and Offshore Structures 15(5): 492-502. DOI: 10.1080/17445302.2019.1661622

Soares-Ramos EPP, Oliveira-Assis L, Sarrias-Mena R, Fernández-Ramirez LM (2020) Current status and future trends of offshore wind power in Europe. Energy 202: 117787. https://doi.org/10.1016/j.energy.2020.117787

Zhang P, Feng J, Shi Y, Le C, Ding H (2024a) Influence of length to diameter ratio of the skirt on horizontal bearing characteristics of tripod suction jacket foundation in sandy soil. Journal of Marine Science and Application 23(2): 406-416. (in Chinese) https://doi.org/10.1007/s11804-024-00411-8

Zhang P, Guo W (2024) Load-bearing characteristics of offshore wind power single column composite bucket foundation under composite loading conditions. Advances in New and Renewable Energy 12(2): 124-132. (in Chinese) DOI:10.3969/j.issn.2095-560X.2024.02.002

Zhang P, Qi X, Zhang C, Le C, Ding H (2023) Penetration tests of multi-bucket foundation in sand for offshore wind turbines. Journal of Ocean University of China 22(4): 949-960. (in Chinese) https://doi.org/10.1007/s11802-023-5304-3

Zhang P, Wang Y, Xiao J, Gao Y (2024b) Investigation into the towing performance of single-column composite bucket foundations. Hydro-Science and Engineering 2024(3): 99-107. (in Chinese) DOI:10.12170/20230308004

Zhang P, Wei Y, Xiao J, Ding H, Li Y (2021) Torsional bearing capacity of composite bucket foundation in silty sand. Acta Energiae Solaris Sinica 42(9): 270-278. (in Chinese) DOI: 10.19912/j.0254-0096.tynxb.2019-0870

Zhang Q, Zhang P (2023) Effect of combined action of scouring and earthquake on the displacement deformation of single-column composite bucket foundation. Advances in New and Renewable Energy 11(6): 548-555. (in Chinese) DOI: 10.3969/j.issn.2095-560X.2023.06.009